



Cathodoluminescence of Powder Layers of Nanometer-Sized $Y_2O_3:Eu$ and Micrometer-Sized $ZnO:Zn$ Phosphor Particles

Daniel den Engelsen, Paul Harris, Terry Ireland,^z Robert Withnall, and Jack Silver^z

Centre for Phosphor and Display Materials, Wolfson Centre for Materials Processing Brunel University, Uxbridge, Middlesex UB8 3PH, United Kingdom

We present a simple method to measure the cathodoluminescence of charging and non-charging phosphor powder layers at low primary electron beam energy. The method is based on comparing a non-charging surface of a conducting material such as copper or indium tin oxide with charging surfaces of non-conducting phosphors. The phosphors that were investigated were $ZnO:Zn$, which is slightly conductive and supposed not to charge upon electron bombardment, and $Y_2O_3:Eu$, which charges at sufficiently high current density. It was found that the luminous efficacies of $ZnO:Zn$ and $Y_2O_3:Eu$ at 5 keV primary beam energy were 23 and 16 lm/w respectively, larger than reported in the literature. This is partly explained by calculating the efficacy from the summation of the luminances measured in the reflected and transmitted mode. This method also minimizes the inaccuracy introduced by the effect of the coating weight. The ratio between luminances measured in reflection and transmission is described in terms of a one-dimensional light scattering theory.

© 2013 The Electrochemical Society. [DOI: 10.1149/2.040309jss] All rights reserved.

Manuscript submitted April 24, 2013; revised manuscript received July 9, 2013. Published July 23, 2013.

Previously we have reported on the various intrinsic luminescent phenomena, such as cathodoluminescence (CL), photoluminescence (PL) of nanometer sized rare earth doped yttrium oxide particles, crystallites and periodic nanostructures for photonic bandgap studies.¹⁻⁵ More recently we have given an account on a CL study on double layers of zinc doped zinc oxide ($ZnO:Zn$) and nanometer sized (NS) europium doped yttrium oxide particles ($Y_2O_3:Eu$).⁶ The objective of that study was to increase the light output of phosphor layers by making double layers of low and high voltage phosphors. In that study it was not possible to show that this approach was successful, mainly because the penetration depth at 5 kV in a thin top layer was insufficient to excite the bottom layer. Other problems were charging of the NS $Y_2O_3:Eu$ top layer, which led to non-reproducible results and focusing effects of the electron beam. In this paper a new method will be introduced for determining the CL efficacy of phosphor powder layers that may charge upon electron bombardment. Furthermore, the optical behavior of the micrometer sized $ZnO:Zn$ and the NS $Y_2O_3:Eu$ particles in terms of a one-dimensional light scattering theory will be described.

The challenge of measuring the CL of insulating phosphor layers at low electron beam energy is that the use of a top layer of aluminum (Al) to prevent charging of the phosphor grains cannot be used. This charging is negative in the case of the secondary emission coefficient γ being <1 , or positive in the case that $\gamma > 1$. In principle the surface potential could approach that of the primary beam, and deflect the incoming beam. In practice no evidence of this happening has been observed in this work. What appears to be happening is that the thin surface layer charges up until it reaches the dielectric breakdown threshold of the material and then discharges, before resuming charging. As a result the surface potential fluctuates rapidly. This behavior can clearly be seen when the specimens are examined in an electron microscope. The breakdown threshold is relatively modest because of the thin nature of the particles and photoconductivity induced in the surface bombarded by the electron beam.

Charging of the phosphor layer makes it very difficult to measure the current striking the sample, because the current is not efficiently collected by the ammeter and it is very difficult to suppress secondary electron emission, which can result in substantial error. To prevent charging in low voltage devices such as vacuum fluorescent displays, transparent conductive particles are added (such as In_2O_3) to the phosphor layer.⁷ However for measuring luminous efficacy, adding conductive particles is not attractive, since it dilutes the phosphor layer with non-emitting material.

For the present study, $ZnO:Zn$ and NS $Y_2O_3:Eu$ was again chosen, because $ZnO:Zn$ is slightly conductive and supposed not to

charge upon electron bombardment, whereas $Y_2O_3:Eu$ is insulating and charges upon electron bombardment.^{6,8,9}

The difficulties in measuring the lumen efficacy and energy efficiency (sometimes called quantum efficiency) of low-voltage phosphors can be appreciated from the spread of published values by Shea,^{10,11} Yang et al.,¹² Wakefield et al.¹³ and Dmitrienko et al.^{14,15} These latter authors stated that charging of $ZnO:Zn$ at low current density is less of an issue, because changes of the CL efficacy of $ZnO:Zn$ may be caused by variations in the surface layer of the grains. Surface contamination or doping of the surface layer with small amounts of n-type oxides increased the luminous efficacy by 200 to 400%. Yang et al. published the lumen efficacy of commercial powders of $ZnO:Zn$ and $Y_2O_3:Eu$ in the range of 0.5–5 kV.¹² These authors and Wakefield et al.¹³ found almost two times larger values for $Y_2O_3:Eu$ than Shea and Walko.¹¹ Charging of $Y_2O_3:Eu$ could be the reason for the rather large spread in the luminous efficacy of $Y_2O_3:Eu$. Varying the bias voltage of sample or shield provides information on the charging condition of a surface that is bombarded with electrons.¹ This measuring method was applied to determine whether our layers were charging or not.

The outline of this paper is as follows. In the experimental section the synthesis of NS $Y_2O_3:Eu$ is described, in addition to methods for measuring the secondary electron (SE) emission and the CL of thin phosphor layers that may be charging upon electron bombardment. Results and a discussion thereof are presented in the subsequent section respectively. The final section contains the conclusions.

Materials and Methods

Materials.— $ZnO:Zn$ phosphor was obtained from Kasei Optonix, Japan and used without further treatment. Y_2O_3 (99.99%), europium oxide (Eu_2O_3 , 99.99%) were obtained from Ampere Industrie, France; urea, ethylenediaminetetraacetic acid (EDTA), nitric acid (HNO_3) and isopropanol (IPA) were supplied by Fisher Scientific, UK., all chemicals were used as received. Glass substrates (1 cm^2) coated with one ITO film ($85\Omega/\text{sq}$) or two ITO films ($40\Omega/\text{sq}$) were obtained from Visiotech Ltd., UK.

Preparation of NS spherical $Y_2O_3:Eu$.— The urea homogeneous precipitation and its modifications were used to prepare various batches of monosized NS spherical amorphous europium-doped hydroxycarbonate particle precursor powders of spherical $Y_2O_3:Eu$ phosphor particles.² To produce these aforementioned phosphors a europium-doped yttrium nitrate [Y and $Eu(NO_3)_3$, 0.25M] stock solution was prepared by dissolving the yttrium and europium oxides in dilute HNO_3 , according to the composition ($Y_{1-x}, Eu_x)_2O_3$, in this work $x = 2.0$ (mol%). This was followed by adjusting to $\sim\text{pH}3$ with

^zE-mail: jack.silver@brunel.ac.uk; terry.ireland@brunel.ac.uk

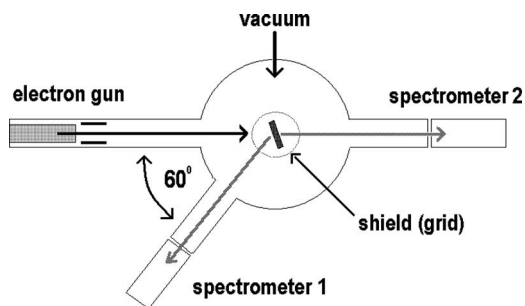


Figure 1. Top view of vacuum chamber, electron gun, sample, shield, spectrometer 1 (reflection mode) and spectrometer 2 (transmission mode).

ammonia solution and made up to one liter by adding de-ionized water. To produce narrow size distribution 300, 400 and 500 nm diameter spherical particles: to a one liter beaker were added de-ionized water (475 mL), $\text{YEu}(\text{NO}_3)_3$ stock solution (25 mL) and urea (15.0g), the solution was heated to boiling on a hotplate and maintained throughout the precipitation. When turbidity was observed the solution was aged for one hour to obtain 300 nm, 90 minutes for 400 nm and two hours for 500 nm particles. To produce 100 and 200 nm diameter particles EDTA (3.0g and 1.5g respectively) was added at the start of the reaction. After the respective aging period the precipitate was immediately filtered at the pump (whilst the solution was still hot), washed three times with de-ionized water and dried in an oven at 80°C . The phosphor precursor particles were then annealed at 980°C in a furnace for six hours to yield the cubic monosized spherical $\text{Y}_2\text{O}_3:\text{Eu}$ phosphor particles.

Characterization.— The morphology and particle size assessment of the phosphor powders were undertaken using a field emission scanning electron microscope (FESEM), Supra 35 VP, Zeiss, Germany.

Phosphor layers were deposited onto the ITO-coated glass slides by settling from iso-propanol suspensions containing various phosphor concentrations. These suspensions were dispersed by ultrasonic cavitation prior to settling. Electrophoretically deposited layers were not studied, since these layers were observed by FESEM studies to have a very rough surface, with large internal voids and strongly light-scattering.⁶

The CL measurements were carried out in a high vacuum chamber at a vacuum level of 5×10^{-6} mbar using a Kimball Physics Inc., USA electron gun (EFG-7) and power supply (EGPS-7). CL measurements were taken over a range of electron beam accelerating voltages from 1 to 5 kV; the system had the ability to focus and defocus the beam over a range of current densities. Deflection plates enabled optimum positioning of the electron beam on the sample. The high vacuum chamber, electron gun set-up and viewing port geometries are shown in Fig. 1. The sample was positioned in the center of the vac-

uum chamber and its vertical position and azimuth angle could easily be changed and optimized. The spectrometers shown in Fig. 1 were spectroradiometers, Spectrobos 1200, JETI, Germany, recording the radiance, luminance and CIE coordinates from the sample between 380 and 780 nm.

Essential to the method described herein is measuring in both reflection and transmission mode. In the reflection mode, the CL is measured at the gun side of the sample, whilst in the transmission mode the luminescence transmitted through the ITO-coated glass slide is measured. The advantage of this measuring method is that the sum of the radiances in the reflection and transmission modes is largely independent of the coating weight for non-absorbing samples. It should be mentioned that measuring CL in reflection and transmission mode was already reported by Brill and Klasens in 1952.¹⁷ However, this method of measuring CL was not developed further.

Since the focus in this paper is on measuring CL of powder layers that may charge upon electron bombardment, the sample holder in the vacuum chamber will be described in detail, because that component is relevant for dealing with charging layers. This measuring method is based on the assumption that a good conducting material such as Cu or ITO does not charge upon electron bombardment. That implies that for these materials it is easier to determine the effective current impinging on the surface. The effective current is the sum of primary electrons hitting the surface and SE leaving from that surface. So, in order to determine the effective current, the SEs must be sent back to the surface to be measured. This can be done by biasing the target surface positively, or using a shield or grid that is biased negatively. The latter method was chosen, because in this way the collection of SEs emitted from the wall of the vacuum chamber could be avoided. In the case of a charging sample, it is not possible to be completely certain that all SEs are collected by biasing the shield. This depends on the charging voltage, which is not easy to measure in combination with a CL-measurement.

In order to deal with this problem, a comparison method was developed: CL from a charging sample was measured by applying the same current settings as used for a non-charging reference surface (Cu or ITO). Copper and ITO were chosen for having similar backscattering yields to $\text{ZnO}:\text{Zn}$. Two measuring methods were devised, which are both depicted in Fig. 2. In Fig. 2a the reference non-charging surface is a Cu plate (as received) and in Fig. 2b it is a glass slide coated on both sides with ITO. In (a) the reference and sample are positioned in the E-beam by a vertical translation and in (b) this is done by rotation through 180° . When making measurements, the reference was firstly positioned in the E-beam, the current was adjusted to $1 \mu\text{A}$ (as indicated by the ammeter), yielding a current density of $1 \mu\text{A}/\text{cm}^2$, since the surface areas of references and samples were 1 cm^2 in all cases. The shield was biased to -50 V ; so that, low energy secondary electron emission from the reference sample was totally suppressed, and thus a true measurement of the current striking the sample was made. The grid structure was designed to have as high a transparency as possible (about 98%) so that high energy backscattered electrons

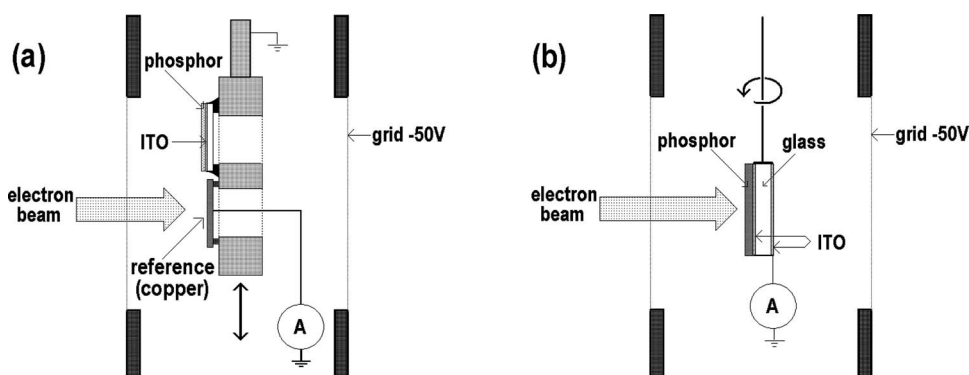


Figure 2. (a): Translation holder made of Al. (b): Rotational sample made of glass, which has thin ITO films on both sides.

(BSEs) were able to escape unhindered: i.e. these were not detected in this way. The sample was maintained at earth potential and so the kinetic energy of the electrons was simply related to the applied cathode voltage. This is not always the case in other studies and for example in the studies by Shea^{10,11} and Wakefield et al.¹³ the sample was biased, and therefore a correction had to be made to calculate the kinetic energy of the primary electrons.

In making CL measurements with charging and non-charging phosphor samples, the current adjustment as determined for the reference surface was not altered. The ITO-layer was connected to earth during the CL-measurements. The assumption was that the same quantity of primary electrons hit the charging phosphor layer as determined for the non-charging reference. Obviously, this is only correct if the voltage due to charging is low as compared to the beam voltage. A comment on this assumption will be made when discussing the SE-yield curves of ZnO:Zn and NS Y₂O₃:Eu.

The electron beam was defocused in such a way that it yielded a uniform spot on the phosphor samples. The luminance uniformity of the spot was visually optimized by adjusting the focus voltage. The focus voltage of the electron gun was about ~45% of the anode voltage in measuring SE yield and CL. At this focus voltage the focusing of the cathode of the gun is in front of the sample (over focus condition), while the luminance distribution from the phosphor samples is uniform. The focus voltage could not be decreased below 40%, because at large over focus conditions a part of the primary electron beam that passed the sample hit the rear side of the shield and created low voltage SEs. These electrons could also be collected by the sample ammeter and would yield an erroneous effective sample current.

Calculation of the lumen efficacy.— The calculation of the luminous efficacy of phosphor layers on ITO coated glass is based on the assumption that the light intensity has a Lambertian distribution. It is furthermore assumed that the distribution of the CL is independent of the particle size and the layer thickness or coating weight. Since a rigorous theory for light scattering and absorption in densely packed phosphor layers does not exist, we shall base the description of the light output on the well-known one-dimensional continuum theory of Kubelka and Munk.¹⁸ This theory was slightly modified by Hamaker¹⁹ in 1947 and used by Brill and Klasens.¹⁷ The luminance L_t in the transmission direction (going to spectrometer 2 in Fig. 1) can be written as

$$L_t = \frac{\Phi}{2\pi A} \left[\frac{1 - r_G}{\frac{a+(1-r_G)s}{\sigma} \sinh \sigma D + \cosh \sigma D} \right] \quad [1]$$

and for the luminance L_r in the reflection direction

$$L_r = \frac{\Phi}{2\pi A} \left[\frac{(1 + r_G) \cosh \sigma D + \frac{(1-r_G)(a+2s)}{\sigma} \sinh \sigma D}{\frac{a+(1-r_G)s}{\sigma} \sinh \sigma D + \cosh \sigma D} \right] \quad [2]$$

where Φ is the total light flux (in lm) produced in the layer, A is the surface area of the sample, r_G is the reflection coefficient of the ITO film, D is the layer thickness, a is the absorption coefficient, s is the scattering coefficient and

$$\sigma = \sqrt{a(a + 2s)} \quad [3]$$

It should be mentioned that we have slightly modified the original equations of Hamaker in terms of luminance instead of intensity. The factor 2 in the denominators of equations 1 and 2 stems from measuring in both reflection and transmission mode: half of the photons generated in the phosphor layer go in the reflection direction (spectrometer 1 in Figure 1), the other half goes in the transmission direction (spectrometer 2). For phosphor layers the absorption coefficient, a , is usually 2 orders of magnitude smaller than s and may be neglected. When $a \rightarrow 0$, then $\sinh \sigma D \rightarrow \sigma D$ and $\cosh \sigma D \rightarrow 1$. Equations 1 and 2 can now be written as:

$$L_t = \frac{\Phi(1 - r_G)}{2\pi A\{(1 - r_G)sD + 1\}}, \quad [4]$$

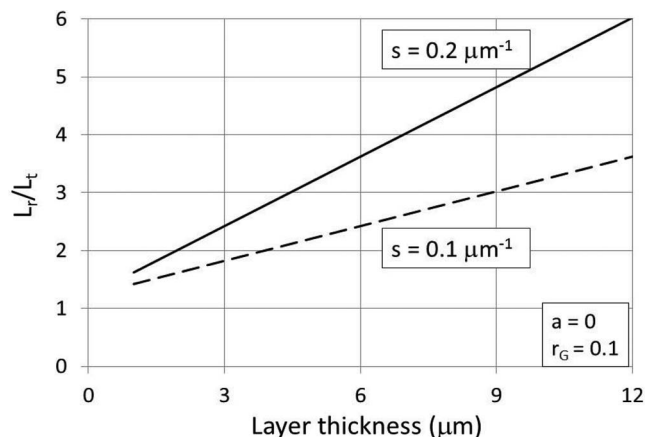


Figure 3. Ratio L_r/L_t versus layer thickness for $s = 0.1$ and $0.2 \mu\text{m}^{-1}$.

and

$$L_r = \frac{\Phi\{1 + r_G + 2(1 - r_G)sD\}}{2\pi A\{(1 - r_G)sD + 1\}} \quad [5]$$

It can easily be verified that for thin non-absorbing layers the sum $L_t + L_r$ is equal to $\Phi/\pi A$, being independent of the layer thickness or coating weight and of the reflection coefficient r_G of the ITO film on glass. The ITO films with a resistance of $85\Omega/\text{sq}$ have a reflectance of 7% at a wavelength of 555 nm and an angle of incidence 30° . Due to the (assumed) Lambertian distribution of the CL, the reflectance of the ITO-film is irrelevant for the calculation of the lumen efficacy and the energy efficiency of the phosphor layers. The ratio L_r/L_t for non-absorbing layers can be written as:

$$\frac{L_r}{L_t} = \frac{1 + r_G + 2(1 - r_G)sD}{1 - r_G} \quad [6]$$

Equation 6 shows that the ratio L_r/L_t is a linear function of the thickness D of the phosphor layer; this behavior is depicted in Fig. 3. The scattering parameters and the reflection coefficient r_G in Fig. 3 are believed to be realistic (average) for our samples.

The luminances L_t and L_r measured outside the vacuum chamber need to be corrected for the reflection losses at the windows of the vacuum chamber: a factor of 1.08 for L_r and a factor of 1.12 (or 1.16 in the case both sides of the glass were coated with ITO) for L_t .

The luminous efficacy η of the phosphor is:

$$\eta = \frac{\Phi}{P} = \frac{\Phi}{jVA} \quad [7]$$

where P is the electric power dissipated in the phosphor layer, j is the current density and V is the voltage of the electron beam. The light flux Φ in equation 7 can only be used if the electrons transfer their kinetic energy completely to the phosphor particles, i.e. if the layers are thicker than the penetration depth of the phosphor. The literature on the penetration depth of electrons in solid materials is extensive.²⁰⁻²³ there is a large variation of the electron range of more than a factor of 3 at 5 kV between the lowest and highest reported value. The formula used by Kanaya and Okayama²³ appears to produce results that are close to the average of other approaches. Using their range formula we calculate a penetration depth of 230 nm at 5 kV for Y₂O₃:Eu and slightly less for ZnO:Zn. Our layers were at least a factor of 10 thicker than this and so we can safely assume that the electrons transferred their kinetic energy to the phosphor.

Equations 1, 2 and 4-6 can also be applied when the luminances L_r and L_t are replaced by the corresponding radiances, R_r and R_t , respectively. From the total radiant power, $2\pi A(R_r + R_t)$, the energy efficiency can be calculated with the radiance equivalent of Eq. 7. The radiance in the transmission mode R_t could not be measured accurately at beam voltages below 3 kV because of interfering light from the filament of the electron gun. At 4 and 5 kV this interference

could be neglected. The luminance measurement did not suffer from this disturbance because of the convolution of the spectral radiance with the eye sensitivity function.

Results and Discussion

Presented in Fig. 4a is a FESEM image of the ZnO:Zn particles before settling on the ITO glass substrate, their particle sizes were shown to be in the range 0.2 to 1.5 μm . In Fig. 4b are shown studies of NS $\text{Y}_2\text{O}_3\text{:Eu}$ powders which were a mixture of batches containing a variety of monosized spherical NS $\text{Y}_2\text{O}_3\text{:Eu}$ particles, these were found to be either discrete, single crystallites of 40 to 80 nm diameter or hollow spheres (150 to 500 nm diameter) formed of crystallites with sizes from 40 to 100 nm. It should be stated that the larger particles are not agglomerates of the smaller NS crystallites; each batch was precipitated as amorphous spherical europium-doped yttrium hydroxycarbonate particles, approximately 20% larger than the final phosphor particles. Upon annealing the amorphous hydroxycarbonates decomposed to the cubic NS $\text{Y}_2\text{O}_3\text{:Eu}$ phosphor, as the crystallites start to grow the precursor hydroxycarbonate particles shrink. The NS $\text{Y}_2\text{O}_3\text{:Eu}$ for our studies was a mixture of various batches with particle sizes ranging from 40 to 500 nm in diameter.

Shown in Fig. 4c is a cross section of a ZnO:Zn layer overlain by a thin $\text{Y}_2\text{O}_3\text{:Eu}$ layer, in Fig. 4d is a higher magnification study of the previous image where both phosphor particles are clearly observed

By measuring the sample current as a function of shield voltage, it was possible to check the efficiency of collecting SEs. The sample current plotted in this way is a relative SE-yield curve; the adjective "relative" refers to adjusting the sample current at $V_{\text{shield}} = -50\text{ V}$ to 1 μA . It was assumed that in this condition and a non-charging phosphor layer, all generated SEs return to the phosphor layer and that the sample current reflects the current of primary electron beam. This assumption is not completely correct, since high-energy elastically backscattered electrons and other BSE are not accounted. However, since these electrons deposit only a small fraction of their energy to the phosphor layer, their effect will be neglected.

The measured sample currents versus V_{shield} have been plotted in Fig. 5 and 6. Figure 5 shows the results for ZnO:Zn and ITO as a function of shield bias voltage. The primary beam energy was 5 keV in Fig. 5a and 1 keV in Fig. 5b. This adjustment of the sample current to 1 μA at $V_{\text{shield}} = -50\text{ V}$ for ZnO:Zn was not changed for the ITO surface in rotating the sample by 180°. The focus voltage of the electron gun was about ~45% of the anode voltage in these experiments. The SE-yield curves for a ZnO:Zn layer with a coating weight of 3.9 mg/cm^2 were almost identical to the curves

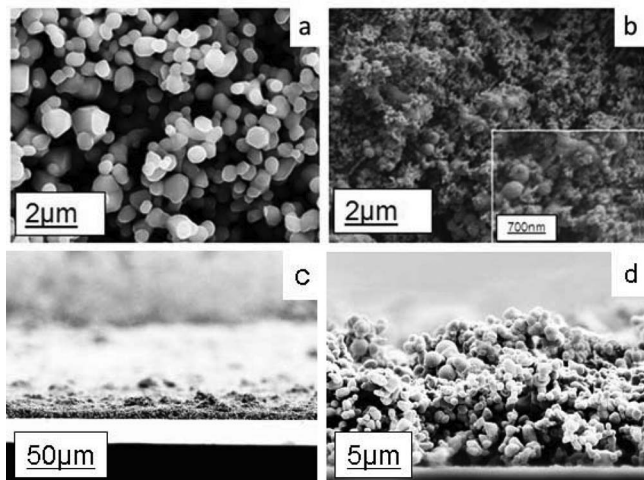


Figure 4. FESEM images of (a) ZnO:Zn particles, (b) $\text{Y}_2\text{O}_3\text{:Eu}$ particles used in this work; (c) is a cross-section through a ZnO:Zn layer overlain by a thin $\text{Y}_2\text{O}_3\text{:Eu}$ layer, (d) is a higher magnification study of (c).

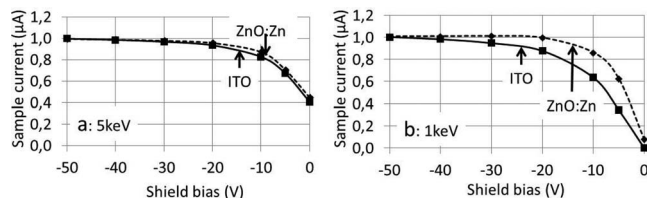


Figure 5. Relative SE-yield curves for ZnO:Zn and ITO at 5 keV (a) and 1 keV (b) primary beam energy. Coating weight was 1 mg/cm^2 and electron beam was defocused.

presented in Fig. 5. Fig. 5b indicates that the sample current for the ITO coated glass was still slightly increasing at a shield bias of -50 V , whereas for ZnO:Zn it was constant. When the reference ITO-surface was thoroughly cleaned after settling, this effect decreased. In Fig. 6a we have plotted the SE-yield curves at various focus voltages for NS $\text{Y}_2\text{O}_3\text{:Eu}$ and ZnO:Zn. The primary beam energy was 3 keV. The sample current was adjusted at $V_{\text{shield}} = -50\text{ V}$ and focus voltage of 1.6 kV to 1 μA : this adjustment was not changed during the measurements shown in this Figure. The effect of focus voltage was substantial for $\text{Y}_2\text{O}_3\text{:Eu}$, as can be seen in Fig. 6a, whereas the SE-yield in the case of ZnO:Zn was independent of the focus voltage. At the best focus voltage of 1.93 kV the diameter of the spot size on the sample was 2.5 mm. The spot size increased to 9 mm at a focus voltage of 1.6 kV. From the curves in Figure 6 we conclude that NS $\text{Y}_2\text{O}_3\text{:Eu}$ is charging negatively. The absolute value of the charge increased when the spot sizes decreased, i.e. when the current density increased. The current density which we applied for measuring the CL was 1 $\mu\text{A}/\text{cm}^2$. At this low current density a linear relationship between luminance and current density was still present as can be seen in Fig. 7: phosphor saturation is out of the question at our measuring conditions.

The CL of thin powder layers of ZnO:Zn and NS $\text{Y}_2\text{O}_3\text{:Eu}$ between 1 and 5 kV primary beam voltage (anode voltage) was measured, Fig. 8 shows the results for ZnO:Zn and Fig. 9 refers to NS $\text{Y}_2\text{O}_3\text{:Eu}$. In Fig. 8 and 9 the sums of L_r and L_t are plotted as function of coating weight. L_r and L_t are the luminances measured in the reflection and

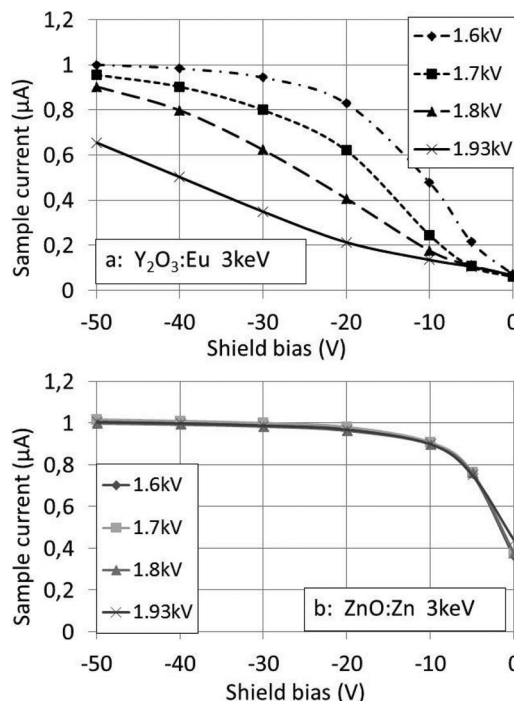


Figure 6. SE-yield curves for 2 mg/cm^2 $\text{Y}_2\text{O}_3\text{:Eu}$ (a) and 2.2 mg/cm^2 ZnO:Zn (b) at 3 keV primary beam energy. Best focus is at 1.93 kV.

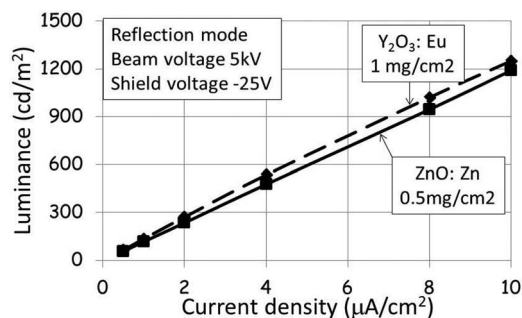


Figure 7. Luminance of ZnO:Zn and NS Y₂O₃:Eu as function of current density at 5 kV anode voltage.

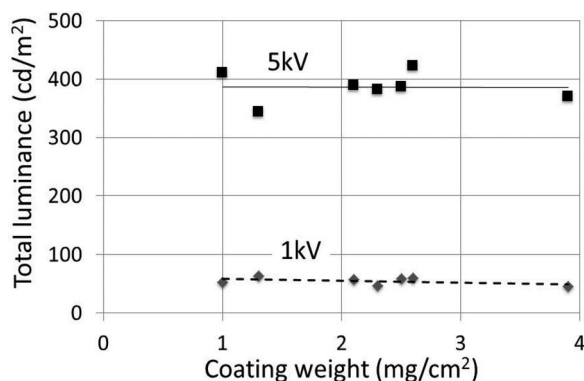


Figure 8. Sum of L_r and L_t for ZnO:Zn at 1 and 5 kV as a function of coating weight.

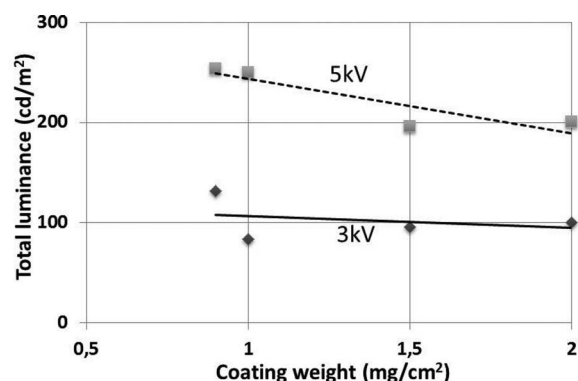


Figure 9. Sum of L_r and L_t for NS Y₂O₃:Eu at 1 and 5 kV as a function of coating weight.

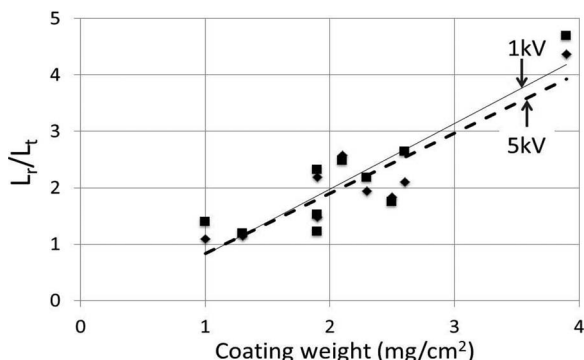


Figure 10. Ratio of L_r over L_t for ZnO:Zn at 1 and 5 kV as a function of coating weight.

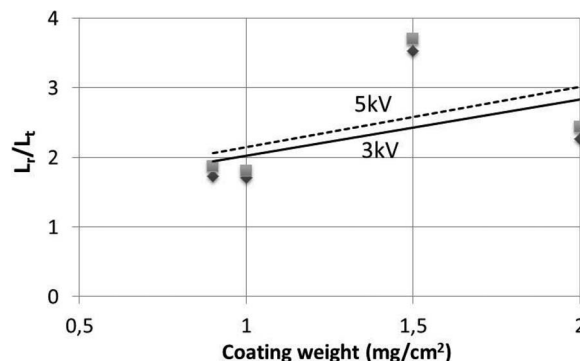


Figure 11. Ratio of L_r over L_t for NS Y₂O₃:Eu at 1 and 5 kV as a function of coating weight.

transmission mode respectively. The constancy of $L_r + L_t$ as a function of coating weight presented in Fig. 8 is in agreement with the one-dimensional scattering theory presented in the previous section. The limited experiments for NS Y₂O₃:Eu represented in Fig. 9 indicate a small decrease of $L_r + L_t$ with coating weight. This observation will be comment upon hereafter.

In Fig. 10 and 11 the ratio L_r/L_t has been plotted as a function of coating weight at 1 and 5 kV anode voltage in Fig. 10 and 3 and 5 kV for Fig. 11. The luminance readings of the spectrometers shown in Fig. 8–11 have been corrected with the reflection corrections at the vacuum windows and the ITO-coated slides as mentioned in section 3. The lumen efficacy of the ZnO:Zn and NS Y₂O₃:Eu layers is represented in Fig. 12 for the samples with ITO films on both sides of the glass slides only. Figs. 8–11 also contain the information of the translational sample holder. The calculation of the lumen efficacy is based on equations 1–7 and the assumption that the sample current for the ITO and Cu reference surfaces at $V_{\text{shield}} = -50$ V represents the CL-relevant current.

The smaller data set used for making the plots presented in Fig. 12 indicated that the lumen efficacy calculated for the highest coating thickness is lower than for the medium coating thicknesses. The average lumen efficacy and energy efficiency for ZnO:Zn and NS

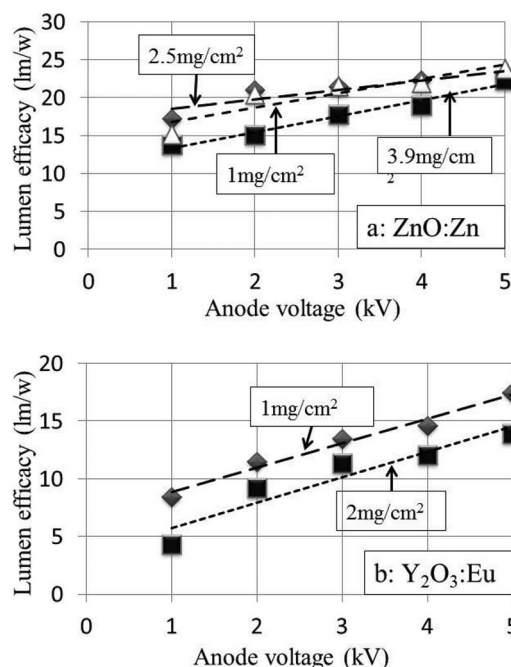


Figure 12. Lumen efficacy as a function of anode voltage for ZnO:Zn (a) and NS Y₂O₃:Eu (b).

Table I. Lumen efficacy, energy efficiency and scattering coefficient for ZnO:Zn and NS Y₂O₃:Eu at 5 kV.

	ZnO:Zn	NS Y ₂ O ₃ :Eu
Lumen eff. (lm/w)	23 ± 2	16 ± 2
Energy eff. (%)	7.1 ± 0.7	5.7 ± 0.6
s (μm ⁻¹)	0.12 ± 0.01	

Y₂O₃:Eu at 5 kV are summarized in Table I. These values are larger than those published previously.^{6,10-15}

The most important cause for this difference is the method to evaluate the lumen efficacy and energy efficiency as explained in Eqs. 1-7: summing the light of the reflection and transmission modes. The results for NS Y₂O₃:Eu of Wakefield are only 30% lower than our values. Yen et al.¹⁶ published a value of 8.7% for the energy efficiency of Y₂O₃:Eu. However, this value does not refer to NS material and the anode voltage is probably much higher than 5 kV.

By repeating an experiment, i.e. settling the phosphor layer onto the ITO-film, mounting the sample in the vacuum chamber and measuring the luminances in the reflection and transmission mode, it was generally possible to reproduce the previous measured values inside a range of ±10%. One important factor for reproducibility was the adjustment of the focus voltage of the electron beam as mentioned in the experimental section. The other one was optimizing the line of sight of the spectrometers to the uniform spot on the sample. The adjustment of the azimuthal angle of the sample in the vacuum chamber (~30°) shown in Fig. 1 only had a minor effect on the reproducibility. Variation of the coating thickness and non-uniform coating thickness in the area of the electron spot affects the individual readings of L_r and L_t; however, the sum L_r+L_t is not affected. This is a major advantage of our measuring method. The larger values of the lumen efficacies (with the uncertainty range taken into account as well) found by us may reflect the fact that in our methodology backscattered electrons are allowed to escape and are not included in the efficacy calculation (because they deposit little energy into the phosphor), whereas other workers may measure the current on the sample using a Faraday cup and in this case the BSE current is included in the total measured current, and this can introduce substantial errors. Similarly, if SE emission is suppressed by simply applying a positive potential to an unprotected sample then substantial errors are introduced due to secondary electrons from elsewhere in the vacuum chamber being drawn onto the sample. These low energy electrons contribute to the measured current but stimulate very little luminescence.

The results published in our previous paper⁶ refer to a stronger over-focus condition, in which a substantial part of the E-beam that passed the sample hit the back side of the shield. The SEs generated at the shield were also collected by the sample: this resulted in too low values (more than a factor of 2) for the lumen efficacy of ZnO:Zn. In the case of NS Y₂O₃:Eu, this difference is less, because of charging. The lumen efficacy of 9 lm/w for NS Y₂O₃:Eu with a coating thickness of 1 mg/cm² at 1 kV agrees quite well with the value of 7.5 lm/w that can be evaluated from measurements made previously in our laboratory.^{2,6}

The behavior of the sample current of the NS Y₂O₃:Eu powder layer shown in Fig. 5a has been visualized in Fig. 13. This Figure demonstrates the effect of focusing the electron beam at constant beam current. In doing so, the current density in the electron spot is increasing and this will increase the negative charging of NS Y₂O₃:Eu. Conductive samples such as ITO and ZnO:Zn collect all SEs at negative bias voltage of the shield, because they are not charging and are at earth potential. Non-conductive layers such as Y₂O₃:Eu can charge either positively or negatively, depending on the SE emission coefficient γ. Wang et al. found a value of 3.8 for γ_{max} of Y₂O₃ at 500 eV primary electron energy.²⁴ At a primary energies >500 V, γ decreases; however, in the range between 1 and 5 keV, γ is still >1.

Thin ITO coatings show a similar behavior; however, γ_{max} is 2.5 at slightly lower primary beam energy of 400 eV.²⁵ At current densities

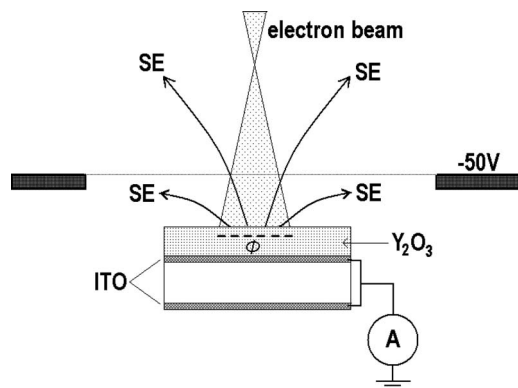


Figure 13. Cross section of sample indicating charging of NS Y₂O₃:Eu at near focus.

between 1 and 10 μA/cm² we assume that the surface potential φ_s of the NS Y₂O₃:Eu layer may be in the range -40 < φ_s < -10 V. The voltage difference between the sample and the shield is much smaller in this case and not all SEs will be sent back to the phosphor surface. The more negative the phosphor gets, the less SEs will be collected by the sample. This reflects exactly the behavior shown in Figure 6a.

It should be mentioned that the sample currents measured at V_{shield} = 0 were very unstable: initially these currents were negative at a primary beam of 1 keV, indicating that the quantity of emitted electrons was larger than the quantity of absorbed electrons. Although, instabilities in the current readings at 5 keV were observed, the initial values of the sample current were higher. This behavior can be explained in terms of a larger γ at 1 keV as compared to that at 5 keV.^{24,25}

The underlying assumption in the new measuring method described above is that the reference non-conducting surfaces, Cu and ITO, collect all primary and SEs at the measuring condition for CL. Only if this condition is met, one can trust the evaluated luminous efficacies. Fig. 5 shows SE-yield curves of non-cleaned ITO-surfaces that are not completely flat at V_{shield} < -25 V. This effect did not disappear completely after thoroughly cleaning of the non-coated ITO film with isopropanol. Besides some charging of the ITO surface due to contamination, there appears to be some other effect operational. One possibility is the 'Malter effect', which has been observed on ITO coated glass in the past.^{26,27} This could arise if the primary electrons penetrate the ITO layer and charge the glass below. It is hard to understand, however, why the low energy Malter electrons would not be suppressed by the field in the same way as normal secondary electrons are. A more plausible explanation may be that local damage (e.g. cracks, scratches) to the ITO coating has resulted in small areas of the slide (e.g. at the corners) that are floating, and that they charge up under the beam and slightly disrupt the suppression field.

As shown in the section on lumen efficacy, the modified Kubelka-Munk theory of the reflection and transmission of light generated in powder layers predicts that at low beam voltage L_r + L_t is independent of coating thickness in the case that the absorption coefficient is zero or very small. If the absorption coefficient cannot be neglected, it is to be expected that L_r + L_t decreases versus coating thickness. This could explain the behavior shown in Fig. 9.

The experimental values of L_r/L_t represented in Figs. 10 and 11 enable us to estimate the scattering coefficients of ZnO:Zn and Y₂O₃:Eu respectively as indicated in Fig 3. This requires a relation between layer thickness and coating weight. Generally the layer thickness D can be expressed as:

$$D = \frac{W}{\rho B} \quad [8]$$

where W is the coating weight, ρ is the density of crystalline phosphor material, 5.6 g/cm³ for ZnO:Zn and 5.0 g/cm³ for Y₂O₃:Eu, and B is the packing density in the layer. An attempt to determine the packing density from SEM pictures recorded at high-tilt angles yielded

an estimated value of about 70%. In a hexagonal close packing of identical spheres the volume fraction of the spheres is 74% and the random close packing density is 64%. Even this latter packing density is seldom obtained in depositing phosphor powder layers. In practice, phosphor layers on TV-screens have packing densities between 55 and 60%. A packing density of 60% for both phosphor layers was assumed. An estimate may be made from Fig. 10 giving a scattering coefficient for ZnO:Zn of $0.12 \mu\text{m}^{-1}$, for Y₂O₃:Eu $\sim 0.12 \mu\text{m}^{-1}$, based on the data for 5 kV in Fig. 11. Because of the limited data points in Fig. 11, this latter value is not inserted in Table I.

The scattering coefficient s was related to the average diameter d_{50} of the phosphor particles in CRT screens with an aluminum-backing layer by Busselt and Raue²⁸ with a phenomenological formula

$$d_{50} = \frac{\sqrt[3]{B}}{s} \quad [9]$$

where B is the packing density. For $B = 0.6$ we find for d_{50} of ZnO:Zn $7 \mu\text{m}$. This is much larger than the real diameter of the phosphor particles used in our work, see Fig. 4a. In other words, Equation 9 is invalid in our case or the one-dimensional scattering theory of Kubelka and Munk cannot correctly describe the optical properties of NS powder layers. We intend to address these issues in a forthcoming study, in which we will extend the CL-measurements to higher anode voltages

Conclusions

Charging of phosphor powder layers upon electron bombardment is a well-known problem in quantitative measurements of CL efficacy, because it makes it difficult to obtain accurate measurements of the current striking the sample. In this work we have developed a simple method to measure the CL of charging phosphor powder layers based upon comparing an unknown sample with a conducting reference that does not charge upon electron bombardment.

Cu plates and ITO coated glass slides were used as non-charging references for adjusting the primary beam current to measure the luminance of ZnO:Zn and Y₂O₃:Eu powder layers. Copper plates gave the most consistent results and cleaning of the reference ITO-surface was found to be critical.

The luminance emitted in forward and reverse (i.e. transmitted and reflected) directions depended strongly on coating weight, and this also complicates quantitative measurements. Summing the luminance obtained from both reflection and transmission measurements provided data that was largely independent of the coating weight, and thus resolved this issue.

We have shown that our data for ZnO:Zn fit to a one-dimensional scattering model with limited light absorption, while in the case nano particle Y₂O₃:Eu: layers the effect of absorption is somewhat larger. The scattering coefficients that were fitted to the experimental results cannot be related to the diameters of the phosphor particles.

The luminous efficacies of ZnO:Zn and Y₂O₃:Eu at 5 keV primary beam energy were found to be 23 and 16 lm/w respectively, which are larger than values reported in the literature. This is partly explained by our method of summing the luminances from reflection and transmission modes, so that all of the emission is included. As discussed, it may also be influenced by the way the backscattered electrons are dealt with in this work, which minimizes the substantial errors that can be introduced in CL investigations.

Acknowledgment

Daniel den Engelsen gratefully acknowledges the hospitality of Professor Jack Silver for being a visiting professor in the Wolfson Center for Materials Processing of Brunel University.

References

1. A. Vecht, C. Gibbons, D. Davies, X. Jing, P. Marsh, T. G. Ireland, J. Silver, and A. Newport, *J. Vac. Sci. Technol. B*, **17**, 750 (1999).
2. X. Jing, T. Ireland, C. Gibbons, D. Barber, J. Silver, A. Vecht, G. Fern, P. Trogwa, and D. Morton, *J. Electrochem. Soc.*, **146**, 4654 (1999).
3. J. Silver, M. I. Rubio-Martinez, T. G. Ireland, G. R. Fern, and R. Withnall, *J. Phys. Chem. B*, **105**, 948 (2001).
4. J. Silver and T. G. Ireland, *J. Mater. Res.*, **19**, 1656 (2004).
5. J. Silver, R. Withnall, T. G. Ireland, G. R. Fern, and S. Zhang, *Nanotechnology*, **19**, 095302 (2008).
6. D. den Engelsen, P. G. Harris, T. G. Ireland, R. Withnall, and J. Silver, *SID Symposium Digest of Technical Papers*, **43**, 861 (2012).
7. W. Yen, S. Shionoya, and H. Yamamoto, Eds, *Phosphor Handbook*, 2nd ed., CRC-Press, Boca Raton, Chapters 6 & 8 (2007).
8. C. H. Seager, W. L. Warren, and R. L. Tallant, *J. Appl. Phys.*, **81**, 7994 (1997).
9. S. H. Cho, S. H. Kwon, J. S. Yoo, C. W. Oh, J. D. Lee, K. J. Hong, and S. J. Kwon, *J. Electrochem. Soc.*, **147**, 3143 (2000).
10. L. E. Shea, *Electrochem. Soc. Interface*, **7**(2), 24 (1998).
11. L. E. Shea and R. J. Walko, *Proc SPIE*, **3636**, 105 (1999).
12. S. Yang, F. Zhang, C. Stoffers, S. M. Jacobsen, C. J. Summers, P. N. Yocom, and S. McClelland, *Proc. SPIE*, **2408**, 194 (1995).
13. G. Wakefield, E. Holland, P. J. Dobson, and J. L. Hutchison, *Adv. Mater.* **13**, 1557 (2001).
14. B. I. Gorfinkel, A. O. Dmitrienko, and V. Ya. Filipchenko, *Inorg. Mater.*, **29**, 1226 (1993).
15. A. O. Dmitrienko and S. L. Shmakov, *Inorg. Mater.*, **30**, 534 (1994).
16. W. Yen, S. Shionoya, and H. Yamamoto, Eds, *Phosphor Handbook*, 2nd ed., CRC-Press, Boca Raton, Chapter 2.9 (2007).
17. A. Brill and H. A. Klasens, *Philips Res. Rep.*, **7**, 401 (1952).
18. P. Kubelka and F. Munk, *Z. Tech. Phys.*, **12**, 593 (1931).
19. H. C. Hamaker, *Philips Res. Rep.*, **2**, 55 (1947).
20. C. Feldman, *Phys. Rev.*, **117**, 455 (1960).
21. T. E. Everhard and P. H. Hoff, *J. Appl. Phys.*, **42**, 5837 (1971).
22. J. D. Kingsley and J. S. Prener, *J. Appl. Phys.*, **43**, 3073 (1972).
23. K. Kanaya and S. Okayama, *J. Phys. D: Appl. Phys.*, **5**, 43 (1971).
24. J. Wang, H. Li, S. Yang, Y. Cui, and M. Zhou, *J. Alloys Compd.*, **379**, 247 (2004).
25. I. L. Krainsky, W. Lundin, W. L. Gordon, and R. W. Hoffman, *Proc. of USAF/NASA Space Craft Charging Conference III*, Colorado Springs, Co., (1980).
26. I. Malter, *Phys. Rev.*, **50**, 48 (1936).
27. J. Olesik and Z. Olesik, *Optica Applicata*, **39**, 903 (2009).
28. W. Busselt and R. Raue, *J. Electrochem. Soc.*, **135**, 764 (1988).